JOURNAL OF CATALYSIS 107, 325–337 (1987)

Partial Oxidation of Propene on Mo–Pr–O Catalysts

J. M. LÓPEZ NIETO, J. L. G. FIERRO, L. GONZÁLEZ TEJUCA, AND G. KREMENIĆ[1]

Instituto de Catálisis y Petroleoquímica, CSIC, Serrano, 119, 28006 Madrid, Spain

Received November 20, 1986; revised April 21, 1987

A study of the propene mild oxidation on Mo–Pr–O catalysts and the characterization of catalysts (with Mo/(Mo + Pr) atomic ratios ranging from 0 to 1) has been carried out. The yield of CO + CO_2 decreased and the selectivity to acrolein and acetaldehyde + acetic acid increased significantly with increasing MoO_3 content up to atomic ratios Mo/(Mo + Pr) = 0.80–0.88. Afterward, the selectivity decreased. The samples are composed of crystalline needles of MoO_3 and agglomerates where Mo and Pr were detected. Pr is present as Pr_6O_{11} in catalysts with low Mo content, this oxide being gradually converted to Pr_2O_3 with increasing MoO_3 loading. It appears that the presence of MoO_3 also has the effect of dispersing the praseodymium oxide. In the catalysts with high Pr content, the reduction rate decreases continuously with time indicating that this process takes place according to the contracting sphere model. However, the catalysts with high Mo content present sigmoidal reduction curves; i.e., they reduce according to the nucleation model. The extent of reduction, for reduction times lower than 0.5 h, decreased with increasing MoO_3 content in the samples. The observed maxima in selectivity for partial oxidation products seem to be due to the higher structural stability of highly disperse Pr_2O_3 relative to Pr_6O_{11} when the latter oxide is mixed with MoO_3 in the above atomic ratios.

INTRODUCTION

In the last years, catalytic oxidation has been the object of an intense study not only because of its theoretical interest but also because of its practical importance. Total oxidation processes have found wide application for the removal of atmospheric pollutants. Partial oxidation products are of great importance in the petrochemical industry. For example, propylene is used in the preparation of polyurethanes and polyesters. Acrolein (a product of propylene oxidation) has been used for the obtention of methionine, glycerol (*1*), and acrylic acid (*2*), of great importance in the production of organic polymers. The introduction of catalysts based in $MoO_3 \cdot Bi_2O_3$ has represented a significant advance in selective oxidation of hydrocarbons. Other systems such as U–Sb (*3*), Sn–Sb (*4*), and Fe–Sb (*5*) oxides have, also, been used for this purpose.

The rare-earth oxides catalyze a variety of reactions such as the isotopic exchange of molecular oxygen with the oxide lattice (*6*), dehydrogenation of alcohols (*7, 8*), oxidation of NO, NO_2 (*9*), H_2 (*10*), propene (*11*), butane (*12*), etc. In this work we modify MoO_3 by addition of a second component (Pr_6O_{11}) to study the effect of the rare-earth oxide in the properties of Mo–Pr–O catalysts. Pr_6O_{11} has been chosen because of its high catalytic activity for oxidation (*12*). To the authors' knowledge, no data on activity and selectivity for oxidation on this binary system are available in the literature. The reactivity of the oxygen in the oxide has been shown to be a factor which plays an important role in the oxidation of hydrocarbons (*13*). Thus, particular attention has been paid to the strength of the bond of lattice oxygen in the different catalyst samples and its influence in total and partial oxidation of propene. Indeed, selectivity to deep oxidation products was found to be high for catalysts containing labile oxygen (Pr_6O_{11}) while formation of acrolein, acetaldehyde, and acetic acid is favored by st ongly bound oxygen. This is clearly seen by the observed disappearance of Pr_6O_{11}

[1] To whom correspondence should be addressed.

0021-9517/87 $3.00

and the simultaneous appearance of small amounts of highly disperse Pr_2O_3 as the Mo content in the samples increases.

EXPERIMENTAL

Materials

The precursors were obtained by evaporation until dryness of solutions of $(NH_4)_6Mo_7O_{24} \cdot 4H_2O$ (Merck, p.a.) and $Pr(NO_3)_3 \cdot 5H_2O$ (Fluka AG, p.a.) in HNO_3 (Merck, reagent grade), at pH 2, in the proper concentrations for a given Mo/(Mo + Pr) atomic ratio. The precipitate was dried overnight at 383 K and then heated in air at 0.15 K min^{-1} up to 823 K and kept at this temperature for 14 h. The composition (atomic ratios Mo/(Mo + Pr)) and the BET specific surface areas (as determined by Kr adsorption at 77 K; Kr cross-sectional area, 0.21 mm^2) of the different catalysts are given in Table 1.

TABLE 1

Composition and Specific Surface Areas of the Mo–Pr–O Catalysts

Catalysts	Atomic ratio Mo/(Mo + Pr)	S_{BET}[a] ($m^2\ g^{-1}$)	Temperature coefficient (kJ $mole^{-1}$)
a	0	8.6	118.7
b	0.09	14.0	116.6
c	0.27	12.8	110.8
d	0.43	7.0	108.7
e	0.80	0.4	117.5
f	0.88	0.5	106.2
g	0.91	0.2	143.4
h	0.95	0.2	—
i	1	1.0	82.3

[a] Kr cross-sectional area, 0.21 nm^2.

Methods

Catalytic activity. Details of the experimental technique used for catalytic activity experiments have been given elsewhere (*14*). The 1-g catalyst samples (particle size between 0.42 and 0.59 mm) were mixed with SiC (of particle size as above) in a ratio catalyst : SiC = 1 : 4 in volume. Experiments were carried out in the interval 573–703 K; the reactants, water and helium were in molar ratios $C_3H_6 : O_2 : H_2O : He = 20 : 30 : 20 : a$ (a, balance to atmospheric pressure). The total flow was 9.16×10^{-2} mole h^{-1} and the contact time $W/F = 20$ $g_{cat.}$ h moles $C_3H_6^{-1}$. Under these conditions no diffusional effects were observed. Blank runs for a reactant mixture of molar composition as above, at 673 K, yielded a total conversion lower than 0.6%. Conversion into product i (x_i (%)), total conversion (x_t (%)), and selectivity to product i (S_i (%)) were defined as

$$x_i = \frac{\text{moles of } i \times \text{No. of C atoms of } i}{\text{moles of } C_3H_6 \times \text{No. of C atoms of } C_3H_6} \times 100$$

$$x_t = \Sigma_{x_i} \qquad S_i = (x_i/x_t) \times 100.$$

Analytical electron microscopy. Analytical electron microscopy measurements were carried out by means of a Philips SEM 505 electron microscope equipped with a Kevex energy-dispersive analyzer for the electron-stimulated characteristic X-ray emission spectroscopy (EDAX). The accelerating voltage was fixed at 100 kV. The powdered samples were dispersed in distilled water by an ultrasonic bath. One drop of the suspension obtained was then deposited on a standard copper grid covered by a carbon film. The morphology of the specimens was examined by scanning electron microscopy (SEM). The finely focused electron beam allowed the analysis of the elemental composition of the samples, either on local points or in selected areas of 3 × 3 mm.

X-ray diffraction. X-ray diffraction pat-

terns of the oxidic (as prepared) and partially reduced catalysts were obtained with a Philips PW 1060 diffractometer operated at 36 kV and 20 mA, using nickel-filtered Cu$K\alpha$ (λ = 0.1582 nm) radiation.

Kinetics of reduction. Kinetics of reduction measurements were carried out in a 2000 Cahn microbalance working under dynamic conditions. Sixty-milligram samples were heated at 773 K in a He stream (50 cm^3 min^{-1}) until a constant weight was obtained and then contacted with H_2 (50 cm^3 min^{-1}) at 773 K. The weight changes were taken as a measure of the extent of reduction (α) of the catalyst since the water readsorption is negligible under these conditions. α was defined as the ratio between the experimental and the theoretical weight loss expected for a quantitative reduction of MoO_3 to MoO_2 and of Pr_6O_{11} to Pr_2O_3. Initial reduction rates were calculated by analytical differentiation at time zero of the integral data fitted to a mathematical equation.

RESULTS AND DISCUSSION

Catalytic Activity

The main products obtained in propene oxidation were CO, CO_2, acrolein, and acetaldehyde; acetic acid and acetone were obtained in small concentrations. Values of $r_{C_3H_6}$ (rate of propene disappearance) as a function of the catalyst composition and temperature are plotted in Fig. 1 ($r_{C_3H_6}$ and products distribution at 703 K for catalysts with atomic ratio Mo/(Mo + Pr) < 0.43 were not measured because the high catalytic activity observed in these cases did not allow a proper temperature control). The catalytic activity decreases for increasing MoO_3 content in the catalyst; this effect becomes more pronounced for increasing reaction temperatures. However, this activity is nearly constant for Mo/(Mo + Pr) ratios between 0.40 and 0.90 showing little pronounced maximum for a ratio of 0.84–0.88. Temperature coefficients obtained from ln $r_{C_3H_6}$ vs $1/T$ Arrhenius plots are given in Table 1 (last column).

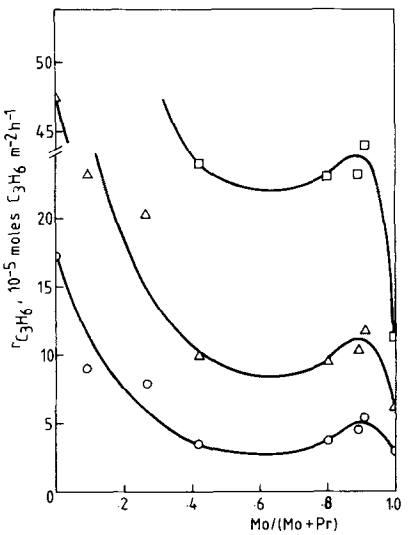

FIG. 1. Reaction rate for oxidation. (○) 643 K, (△) 673 K, (□) 703 K.

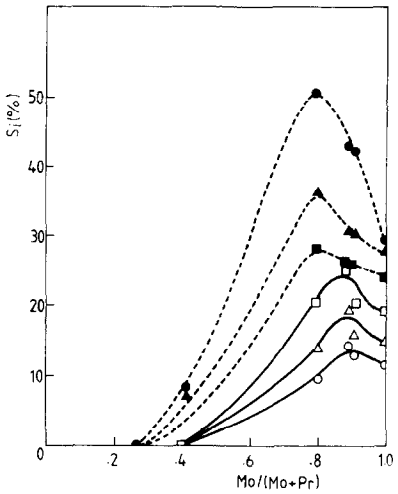

FIG. 2. Selectivity to acrolein (solid lines) and acetaldehyde + acetic acid (dashed lines). (○, ●) 643 K, (△, ▲) 673 K, (□, ■) 703 K.

Selectivities to acrolein, acetaldehyde + acetic acid, and CO + CO_2 as a function of the catalyst composition and reaction temperature are given in Figs. 2 and 3. The yield of CO + CO_2 is 100% for Pr_6O_{11} at 673 K and decreases remarkably for increasing MoO_3 content. The ratio CO/CO_2 presents a maximum for catalysts with Mo/(Mo + Pr) = 0.80–0.88 for the three temperatures studied. The selectivity to acrolein and ac-

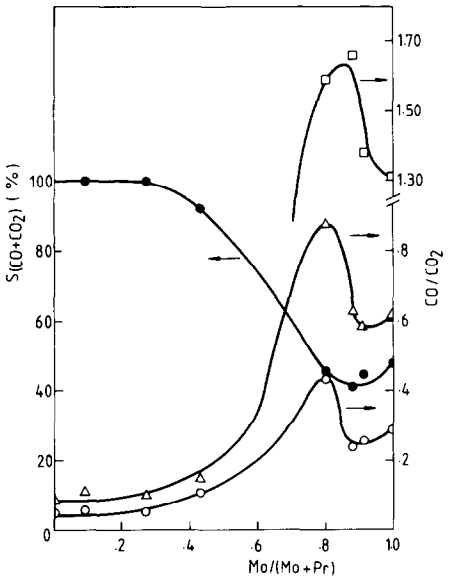

FIG. 3. Selectivity to CO + CO_2 at 673 K (●). CO/CO_2 ratios: (○) 643 K, (△) 673 K, (□) 703 K.

etaldehyde + acetic acid is negligible for catalyst of Mo/(Mo + Pr) ≤ 0.43. However, it increases significantly for catalysts with higher MoO_3 content showing maxima for Mo/(Mo + Pr) = 0.80–0.88. The fact that the position of maxima for CO/CO_2 ratio is practically coincident with maxima for partial oxidation products is consistent with previous data of propene oxidation on SiO_2-supported MoO_3–Pr_6O_{11} catalysts which showed that CO is a secondary oxidation product (*15*). This suggests that CO should be produced by oxidation of acrolein or acetaldehyde.

SEM and EDAX Analyses

SEM and EDAX micrographs of some representative Mo–Pr–O catalysts are given in Fig. 4 (samples will be referred to as in Table 1). Catalysts b and d are composed by agglomerates with Pr as main component and Mo in low concentrations. Catalyst e presents crystalline needles which are characteristic of MoO_3 and agglomerates where Mo and Pr were detected. Catalyst f (not shown) gave micrographs similar to those of e, the difference being that in the former Pr was detected in the agglomerates in very low concentrations. It is seen in this series of micrographs that the Mo–Pr–O catalysts are composed by a part formed by crystallized needles of MoO_3 and a part of agglomerates composed of Mo and Pr, the former decreasing and the latter increasing in concentrations with increasing Pr content in the catalyst. This is consistent with the fact that the specific surface areas observed in the catalysts where Pr is the main component (a–d, Table 1) are remarkably higher (by more than a factor of 10) than the areas of the catalysts with higher Mo content (e–i). Catalyst a (Pr_6O_{11}) has a specific surface area lower than that of catalysts b and c. This supports the view that the presence of MoO_3 has the effect of dispersing the praseodymium oxide through formation of the Mo–Pr phase. The presence of phases composed only of Pr was not detected even in catalyst b with a high content in praseodymium oxide.

X-Ray Diffraction

X-ray diffraction patterns of some catalysts of the Mo–Pr–O series are given in Fig. 5. Pattern a corresponds to Pr_6O_{11}. Pattern b contains peaks of Pr_6O_{11} and peaks of low intensity of Pr_2O_3 indicating that a fraction of Pr_6O_{11} is transformed into Pr_2O_3. This phenomenon is clearly seen in patterns b, c, and d, where peaks of Pr_6O_{11} and Pr_2O_3 decrease and increase in intensity, respectively, as the MoO_3 content in the catalyst increases (Mo/(Mo + Pr) ratio changes from 0.09 to 0.43). This clearly shows that Pr_2O_3 is structurally more stable than Pr_6O_{11} when MoO_3 is added to the latter.

Further addition of MoO_3 causes a profound structural change in the catalyst. Thus, patterns e (not shown) and f (of samples with Mo/(Mo + Pr) = 0.80–0.88) are substantially different from the previous ones: Peaks of MoO_3 and peaks of low intensity of Pr_2O_3 were found. No significant differences were observed between these patterns, similarly to that found in the corresponding SEM micrographs of the re-

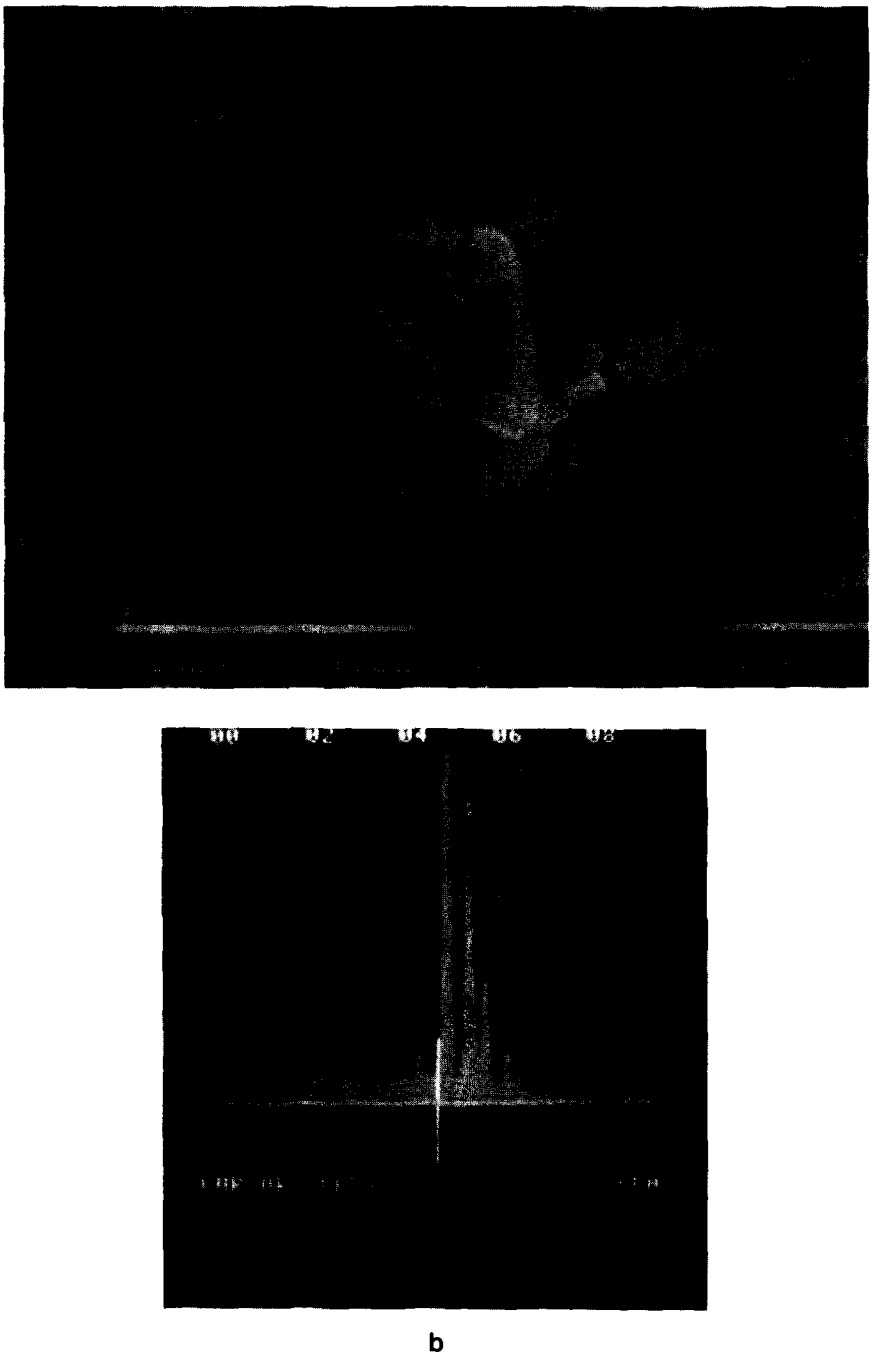

b

FIG. 4. SEM (top) and EDAX (bottom) micrographs for catalysts with variable atomic ratio, r = Mo/(Mo + Pr). Magnification, 4.02 × 10^3. Samples as in Table 1.

spective samples. Pattern i corresponds to molybdite (MoO_3).

X-ray diffraction patterns for the reduced samples, c_r, d_r, e_r, and f_r are given in Fig. 6. These samples are c, d, e, and f after being used in the experiments of kinetics of reduction at 773 K in 50 cm^3 min^{-1} H_2 flow (times of reduction can be found in Fig. 7;

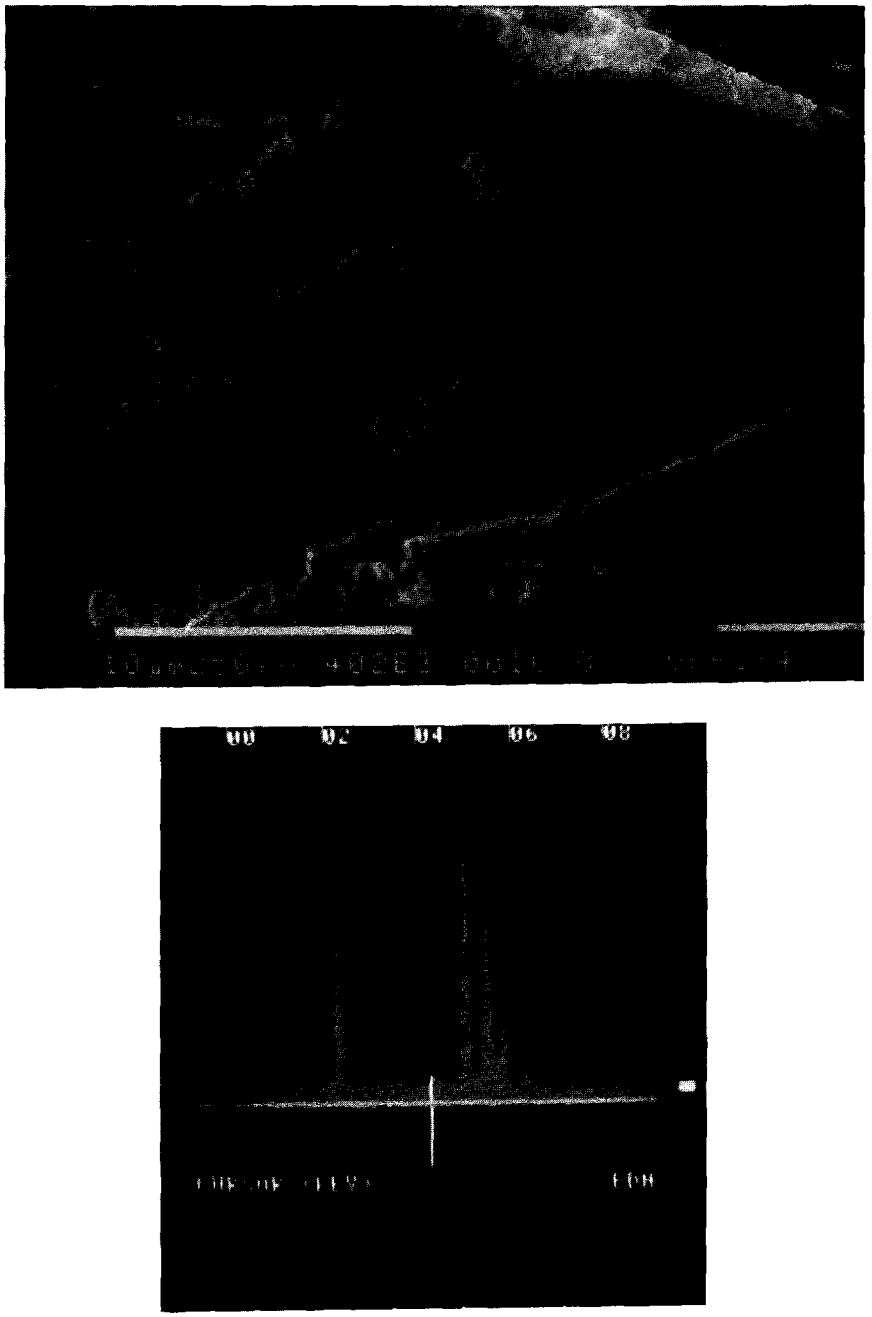

d

FIG. 4—*Continued.*

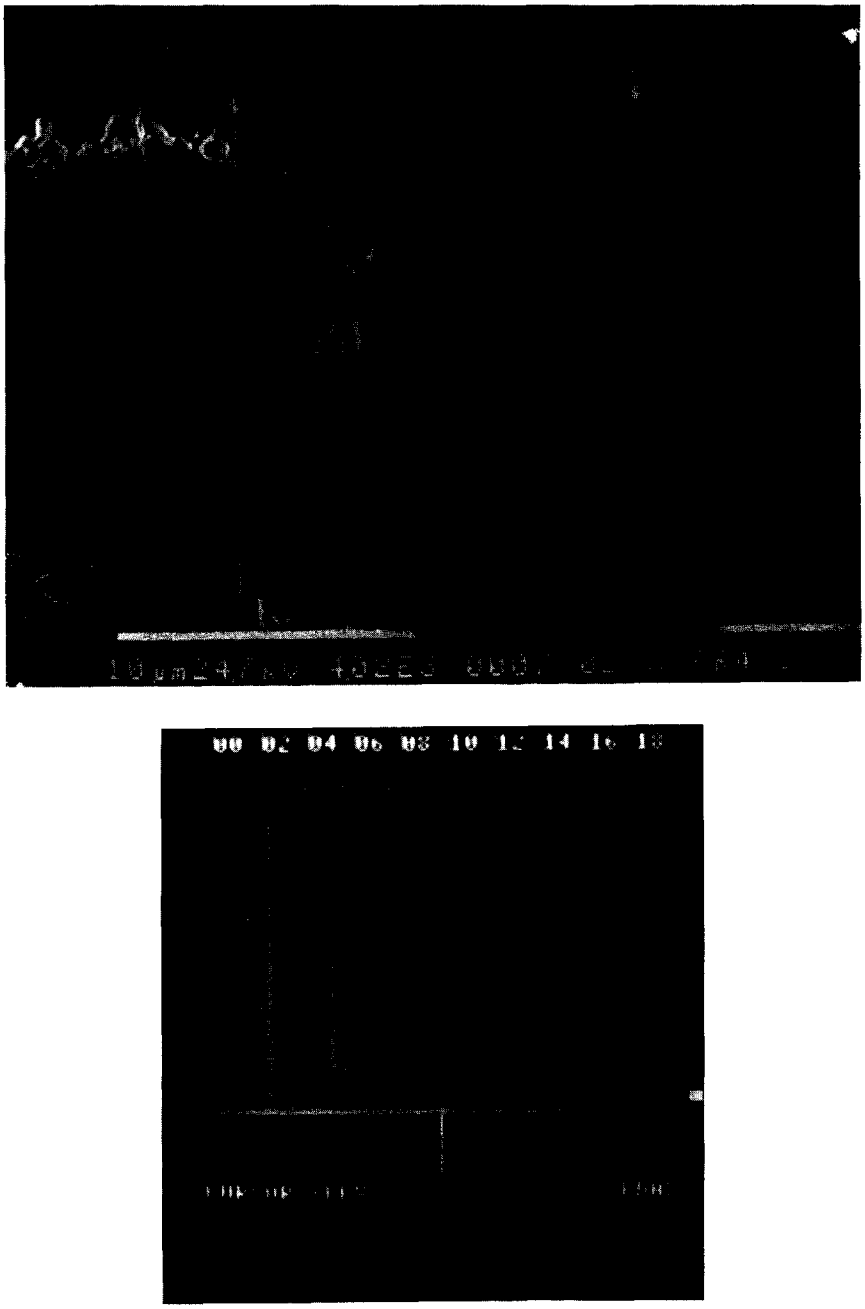

e

FIG. 4—*Continued.*

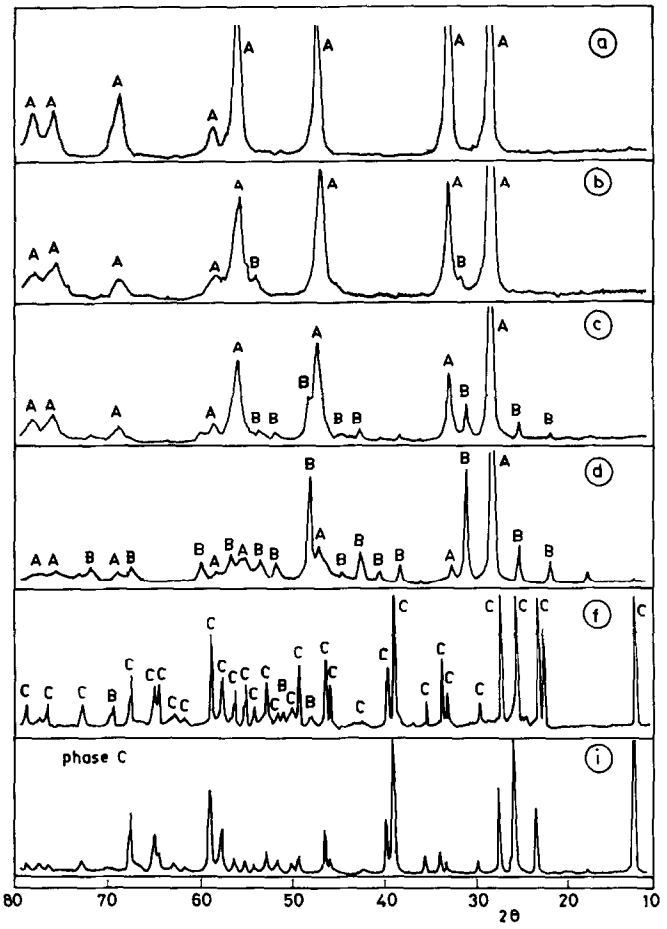

FIG. 5. X-ray diffraction patterns for oxidized (as-prepared) catalysts. Samples as in Table 1. (A) Pr_6O_{11}, (B) Pr_2O_3, (C) MoO_3.

time of reduction for sample e_r was 3 h). Patterns c_r and d_r contain only peaks of Pr_2O_3, these being more intense in the former. This indicates that reduction of Pr_6O_{11} has been more complete in sample c than in sample d. Pattern e_r includes peaks of Mo_4O_{11}, MoO_2, and Mo. The presence in pattern f_r of peaks of unreduced MoO_3 besides peaks of Mo_4O_{11}, MoO_2, and Mo indicates that reduction in sample e has been more profound than in sample f.

Kinetics of Reduction

Curves of kinetics of reduction under isothermal conditions (773 K) for the Mo–Pr–O catalyst series are plotted in Fig. 7. The shape of the curves depends on the atomic ratio Mo/(Mo + Pr). While in the catalysts with a high Pr content (a, b) the reduction rate decreases continuously with time, the catalysts with high Mo content (d, f, h, i) present sigmoidal reduction curves. This suggests that reduction takes place through two different mechanisms. Reduction of the Pr-rich catalysts (Mo/(Mo + Pr) < 0.27) takes place according to the contracting sphere model (*16*) where the process starts with a very fast nucleation which results in a total coverage of the catalyst grains (Pr_6O_{11}) by a thin layer of the reduced phase (Pr_2O_3). This causes a continuous decrease in the reaction rate in the interface Pr_6O_{11}–Pr_2O_3 as the grains of the starting oxide are consumed in the reaction. Reduction of the

catalysts with high Mo content (Mo/(Mo + Pr)) $\geq$ 0.43 takes place according to the nucleation model: First, the reduction rate increases because of the slow growth of nuclei already formed and the appearance of new ones. In the inflection point, the reduced nuclei overlap and the reduction starts advancing from the surface to the bulk. From this point on, the interface of oxidized–reduced phases starts decreasing and so does the reduction rate. The reduction curve yielded by the catalyst with a ratio of Mo/(Mo + Pr) = 0.27 (c) is a combination of the characteristic curves produced by the contracting sphere model (reduction of Pr_6O_{11}) and the nucleation model (reduction of MoO_3). These reduction processes are described, respectively, by the contracting cube equation (*17*), $1-(1-\alpha)^{1/n} = kt$, and by the Avrami–Erofeev equation $1-\alpha = \exp(-kt^n)$, where n and k are temperature-dependent constants.

The reduction degree (α) is an important factor which is a function of the composition of the catalyst. Thus, Pr-rich catalysts (Mo/(Mo + Pr) $\leq$ 0.9; a, b) reach a high reduction degree in comparatively short times, e.g., values of α of 0.5–0.7 were measured at reduction times below 1 h. At higher t, α increases very slowly. On the contrary, Mo-rich catalysts (Mo/(Mo + Pr) $\geq$ 0.88; f, h, i) are reduced at a much lower

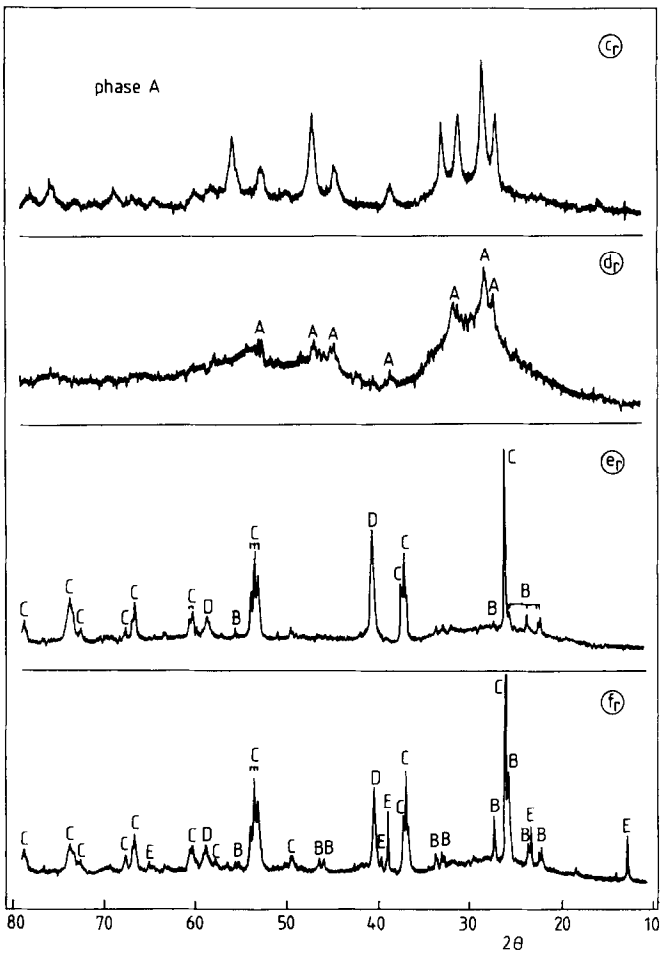

FIG. 6. X-ray diffraction patterns for reduced catalysts (reduction as in Fig. 7). Samples as in Table 1. (A) Pr_2O_3, (B) Mo_4O_{11}, (C) MoO_2, (D) Mo, (E) MoO_3.

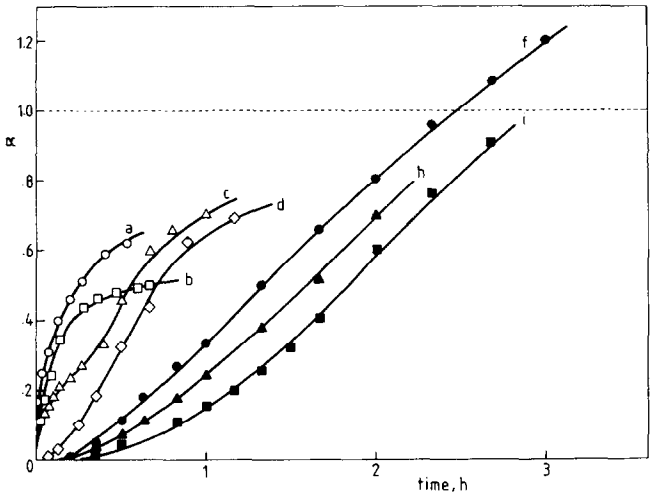

FIG. 7. Kinetics of reduction in a flow of 50 cm^3 min^{-1} H_2 at 773 K. Samples as in Table 1.

reduction rate, and consequently α increases very slowly throughout the period studied (3 h); after this time, the reduction rate does not tend to zero as rapidly as in samples with high Pr content. On the other hand, these Mo-rich catalysts reach higher reduction degrees ($\alpha \geq 1$) than samples with lower Mo concentration, for reduction times $t \geq 3$ h. This indicates that molybdenum in reduced MoO_3 has an oxidation state lower than 4+ in accordance with X-ray diffraction results which showed that metallic Mo, besides MoO_2 and Mo_4O_{11}, is present in e_r and f_r samples (Fig. 6). The samples with ratios $0.27 \leq Mo/(Mo + Pr) \leq 0.43$ (c, d) exhibit a behavior which is intermediate between the two situations mentioned above. The extent of reduction, as measured by α, decreases with increasing MoO_3 content in samples with both low ($Mo/(Mo + Pr) < 0.27$) and high ($Mo/(Mo + Pr) > 0.43$) concentrations in MoO_3. This is consistent with X-ray diffraction results.

The initial reduction rates (r_0) as a function of the ratio Mo/(Mo + Pr) have been calculated and represented in Fig. 8. It is observed that two different reduction processes occur: a very fast one for catalysts where $0 \leq Mo/(Mo + Pr) \leq 0.27$ and a very slow one for catalysts with $0.43 \leq Mo/(Mo + Pr) \leq 1$. The intermediate behavior, mentioned above, is also seen for catalysts with ratios $0.27 \leq Mo/(Mo + Pr) \leq 0.43$. The straight line connecting the initial reduction rates of the pure components (Pr_6O_{11} and MoO_3) would indicate the ideal behavior which would be followed if the r_0 values in the Mo–Pr–O catalysts were additive rates of the pure components. The departure of the experimental r_0 values from this line shows the inhibiting effect in the initial reduction rate of Pr_6O_{11} exerted by MoO_3 for $Mo/(Mo + Pr) \leq 0.27$. This effect is much more marked in catalysts with atomic ratios $Mo/(Mo + Pr) \geq 0.43$, be-

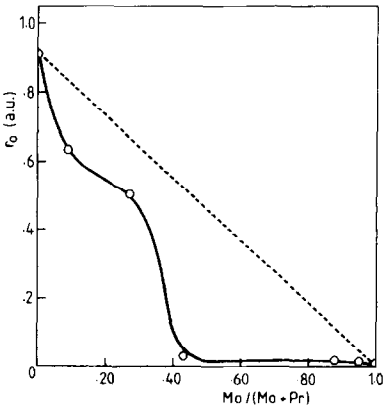

FIG. 8. Initial reduction rates as a function of the ratio Mo/(Mo + Pr).

cause of the gradual conversion of Pr_6O_{11} into Pr_2O_3 (see Fig. 5).

Final Remarks

In general, total oxidation is favored on catalysts with lattice oxygen of a high reactivity, weakly bound to the surface (*18*). On the contrary, partial oxidation is more likely to occur on catalysts with lattice oxygen of a lower reactivity. Pr_6O_{11} has unstable lattice oxygen of a high mobility, probably because of its defective structure (between those of Pr_2O_3 and PrO_2) (*19–22*). Therefore, it falls within the first category. In accordance with this, Pr_6O_{11} exhibits a high rate of exchange with molecular oxygen (*18*).

A measure of the strength of the bond of surface oxygen with the lattice is the heat of formation of the oxide per gram-atom of oxygen (ΔH_{M-O}). In agreement with the above considerations, Morooka *et al.* (*23, 24*) found the more active oxides for total oxidation of hydrocarbons to be those with lower ΔH_{M-O}. Pr_6O_{11} has a low heat of formation (*12*) and this explains its tendency to form deep oxidation products.

However, an alternative form of measuring the strength of the surface oxygen bond is through reduction studies. ΔH_{M-O} will be smaller (larger) for catalysts which are easier (more difficult) to reduce. It is seen in Fig. 7 that the reducibility (as measured by the reduction degree, α) for reduction times lower than 0.5 h decreases with increasing Mo/(Mo + Pr) ratios. In this same direction, the selectivity to CO_2 decreases and the selectivity to partial oxidation products increases (Figs. 1–3). Similar correlations among reducibility, conversion, and selectivity were found by Sachtler and De Boer (*25*) in propene oxidation on a series of metallic molybdates and, also, by Germain and Pérez (*26*) in propene oxidation on metallic oxides.

These results are closely related to those reported by Trifiró *et al.* (*27*). These authors found that the most selective catalysts (within a series of molybdates) for propene oxidation are those exhibiting the lowest diffusion rate of lattice oxygen. Oxygen may be removed by diffusion of oxygen ions from the metal oxide to the interface reduced phase–gas (*16*) in the Mo–Pr–O catalysts used in this study. Thus, the diffusion rate of oxygen will be lower and the selectivity will be higher for catalysts with lower reduction rates, i.e., those with higher Mo/(Mo + Pr) ratios, as it effectively occurs.

Although the experimental results described further confirm the influence of the reactivity of lattice oxygen, it is firmly established that other factors play an important role in propene selective oxidation. Considerable evidence indicates that acrolein formation takes place through a symmetrical allyl intermediate and subsequent insertion of oxygen (*28*). This occurs by interaction of the hydrocarbon and oxygen with a reduction site and an oxidation site, respectively, through a redox cycle. The catalyst bulk structure and the activation of both reacting molecules are, therefore, parameters which greatly influence the overall oxidation process.

Selectivity to acrolein, acetaldehyde, and acetic acid increases for increasing Mo/(Mo + Pr) ratios in the catalysts and exhibits a maximum for ratios of 0.80–0.88 (Fig. 2). Formation of appreciable amounts of acetaldehyde and acetic acid should take place by a different mechanism from that involved in acrolein formation (allylic intermediate). Portefaix *et al.* (*29*), based on labeled propene experiments, demonstrated that the C–C cleavage to yield acetaldehyde does occur at the C=C double bond, by simultaneous interaction of propene with two oxygen atoms, also giving formaldehyde which is readily oxidized to CO_2. The attack at the double bond was also evidenced by Cant and Hall (*30*) in the study of olefin oxidation on supported iridium. The difference between selective oxidation to yield acrolein and complete oxidation (the degradation process) lies in the reactivity of the oxygen species responsible for their

conversion (*13*): Nucleophilic oxygen would lead to allylic oxidation and electrophilic oxygen to degradation products.

Praseodymium is present as Pr_6O_{11} in the catalysts with low ratios Mo/(Mo + Pr) as shown by X-ray diffraction (patterns a–d, Fig. 5). Pr_6O_{11} is gradually converted to Pr_2O_3 with increasing MoO_3 content. In samples with Mo/(Mo + Pr) = 0.80–0.88, the presence of Pr_6O_{11} was not detected; all the praseodymium was in the form of Pr_2O_3. This oxide, as all the sesquioxides of rare earths, is very difficult to reduce (*31*) and its oxygen has a low mobility. These characteristics favor propene oxidation to partial oxidation products. On the other hand, Pr_2O_3 is in low concentrations in these catalysts but it is in a state of higher dispersion than MoO_3 as shown by scanning electron microscopy micrographs (Fig. 4). This disperse phase of Pr_2O_3 should be responsible for the maxima observed in selectivity. The decrease in concentration and eventual absence of Pr_2O_3 in catalysts with Mo/(Mo + Pr) > 0.88 cause the observed decrease in selectivity (Fig. 2).

CONCLUSIONS

A new catalytic system, Mo–Pr–O, has been used for propene oxidation. The catalytic activity first decreased for increasing MoO_3 content and then showed a maximum for an atomic ratio Mo/(Mo + Pr) = 0.84–0.88. The selectivity to acrolein and acetaldehyde + acetic acid increased significantly for increasing MoO_3 content showing maxima for Mo/(Mo + Pr) = 0.80–0.88. SEM and EDAX analyses showed the more active and selective catalysts to be composed of crystalline needles of MoO_3 and agglomerates containing Mo and Pr. The presence of MoO_3 has the effect of dispersing the praseodymium oxide through formation of the Mo–Pr phase. XRD patterns showed that Pr_6O_{11} is gradually transformed into Pr_2O_3 with increasing MoO_3 content in the samples. This indicates that Pr_2O_3 is structurally more stable than Pr_6O_{11} when MoO_3 is added to the latter. In the more active catalysts all the praseodymium is present as Pr_2O_3.

Reduction with H_2 of Pr_6O_{11} and MoO_3 takes place according to the contracting sphere and the nucleation models, respectively. These two models are operative in the reduction of Mo–Pr–O catalysts. MoO_3 exerted an inhibiting effect in the initial reduction rate of praseodymium oxide. This was found to be related to the conversion of Pr_6O_{11} into Pr_2O_3. These results strongly suggest that Pr_2O_3 is responsible for the maxima observed in catalytic activity and selectivity. Formation of acrolein is favored by strongly bound lattice oxygen.

ACKNOWLEDGMENTS

The authors are indebted to CSIC and CAICYT for sponsorship of this work (Project No. 120). Thanks are also due to Dr. J. Martí of Empetrol, S.A., for obtaining analytical electron microscopy micrographs.

REFERENCES

1. Schoel, G. E., *Hydrocarbon Process.* **52,** 218 (1973).
2. Ohara, T., Hirai, M., and Shimizu, N., *Hydrocarbon Process.* **51,** 85 (1972).
3. Callahan, J. L., and Gertisser, B., U.S. Patents 3,198,750 (1965) and 3,308,151 (1967).
4. Barclay, J. L., Bethell, J. R., Bream, J. B., Hadley, D. J., Jenkins, R. B., Stewart, D. G., and Wood, J., British Patent 864,666 (1960).
5. Yoshino, T., Saito, S., Sasaki, Y., and Nakamura, Y., U.S. Patent 3,657,155 (1972).
6. Minachev, Kh.M., and Antoshin, G. W., *Dokl. Akad. Nauk. SSSR* **161,** 122 (1965).
7. Tolstopyatova, A. A., Tsi-tsuan', Y., and Gorshkova, L. S., *Kinet. Katal.* **6,** 466 (1965).
8. Kremenić, G. and Díaz-Soler, J. M., *An. R. Soc. Esp. Fís. Quím.* **65,** 981 (1969); **67,** 1067 (1971).
9. Matsuda, Y., Nishibe, S., and Takasu, Y., *React. Kinet. Catal. Lett.* **2,** 207 (1975).
10. Antoshin, G. W., Minachev, Kh.M., and Dimitriev, R. V., *Izv. Akad. Nauk. SSSR Ser. Khim.* 1864 (1967).
11. Minachev, Kh.M., Kontratev, D. A., and Antoshin, G. N., *Kinet. Katal.* **8,** 131 (1967).
12. Hattori, T., Inoko, J. I., and Murakami, Y., *J. Catal.* **42,** 60 (1976); Takasu, Y., Nishibe, S., and Matsuda, Y., *J. Catal.* **49,** 236 (1977).
13. Kubokawa, Y., and Ono, T., *Bull. Chem. Soc. Japan* **51,** 3435 (1978).
14. Kremenić, G., Nieto, J. M. L., Tascón, J. M. D.,

and Tejuca, L. G., *J. Chem. Soc. Faraday Trans. 1* **81,** 939 (1985).
15. Nieto, J. M. L., Ph.D. thesis, Universidad Autónoma, Madrid, 1985.
16. Hurst, N. W., Gentry, S. J., Jones, A., and McNicol, B. D., *Catal. Rev. Sci. Eng.* **24,** 233 (1982).
17. Keattch, C. J., and Dollimore, D., "An Introduction to Thermogravimetry," 2nd ed., Chap. 5. Heyden, London, 1975.
18. Klissurski, D. G., "Proc. Climax Third Intern. Conf. on the Chemistry and Uses of Molybdenum" (H. F. Barry and P. C. H. Mitchell, Eds.), p. 123. Climax Molybdenum Co., Ann Arbor, MI, 1979.
19. Minachev, Kh.M., "Proceedings, 5th International Congress on Catalysis, Palm Beach, 1972" (J. W. Hightower, Ed.), North-Holland, Amsterdam, 1973.
20. Takasu, Y., Matsui, M., Tamura, H., Kawamura, S., Matsuda, Y., and Toyoshima, I., *J. Catal.* **69,** 51 (1981).
21. Takasu, Y., Matsui, M., and Matsuda, Y., *J. Catal.* **76,** 61 (1982).
22. Takasu, Y., Matsui, M., and Matsuda, Y., *J. Catal.* **98,** 568 (1986).
23. Morooka, Y., and Ozaki, A., *J. Catal.* **5,** 116 (1966).
24. Morooka, Y., Morikawa, Y., and Ozaki, A., *J. Catal.* **7,** 23 (1967).
25. Sachtler, W. M. H., and De Boer, N. H., "Proceedings, 3rd International Congress on Catalysis, Amsterdam, 1964" (W. M. H. Sachtler, G. C. A. Schuit, and P. Zwietering, Eds.), Vol. 1, p. 252. Wiley, New York, 1965.
26. Germain, J. E., and Pérez, R., *Bull. Soc. Chim. France* 4683 (1972).
27. Trifiró, F., Centola, P., Pasquon, I., and Jiru, P., "Proceedings, 4th International Congress on Catalysis, Moscow, 1968" (B. A. Kazansky, Ed.), Vol. I, p. 252. Adler, New York, 1968.
28. Keulks, G. W., Krenzke, L. D., and Notermann, T. M., *in* "Advances in Catalysis" (D. D. Eley, H. Pines, and P. Weisz, Eds.), Vol. 27, p. 183. Academic Press, New York, 1978.
29. Portefaix, J. L., Figueras, F., and Forissier, M., *J. Catal.* **63,** 307 (1980).
30. Cant, N. W., and Hall, W. K., *J. Catal.* **27,** 70 (1972).
31. Topp, N. E., *in* "Chemistry of the Rare-Earth Elements," Elsevier, Amsterdam, 1965.